Int. J. Heat Mass Transfer. Vol. 30, No. 6, pp. 1037–1049, 1987
Printed in Great Britain

0017–9310/87 $3.00 + 0.00
Pergamon Journals Ltd.

Moisture transport in silica gel packed beds—I. Theoretical study

AHMAD A. PESARAN† and ANTHONY F. MILLS
School of Engineering and Applied Science, University of California, Los Angeles, CA 90024, U.S.A.

(*Received* 28 *March* 1986 *and in final form* 29 *July* 1986)

Abstract—Diffusion mechanisms of moisture within silica gel particles are investigated. It is found that for microporous silica gel surface diffusion is the dominant mechanism of moisture transport, while for macroporous silica gel both Knudsen and surface diffusions are important. A model is proposed for simultaneous heat and mass transfer in a thin packed bed of desiccant particles, which accounts for diffusion of moisture into the particles by both Knudsen and surface diffusions. Using finite difference methods to solve the resulting partial differential equations, predictions are made for the response of thin beds of silica gel particles to a step change in air inlet conditions, and compared to a pseudo-gas-side controlled model commonly used for the design of desiccant dehumidifiers for solar desiccant cooling applications.

1. INTRODUCTION

SILICA gel desiccant is widely used in industrial drying processes: generally the beds are relatively thick and can be designed using quasi-steady breakthrough methods. In recent years silica gel has been considered for solar powered evaporative desiccant air conditioning systems, for which pressure drop constraints require use of thin beds (< 15 cm thick). The operation of thin beds is inherently transient and current design procedures are based on models of the transient heat and mass transfer occurring in the bed. Such models represent the overall heat and mass transfer from the air stream to the silica gel by pseudo-gas-side transfer coefficients following the early example of Bullock and Threlkeld [1].

Clark *et al.* [2] tested a prototype scale bed designed for solar air conditioning applications and found rather poor agreement with predictions based on the pseudo-gas-side controlled model, particularly after a step change in inlet air condition. They concluded that the discrepancy was due to shortcomings of the model, since the solid-side mass transfer resistance exceeded the gas-side resistance under these conditions. The experimental data reported by Clark *et al.* was somewhat limited and imprecise since the bed was a large prototype design: hence Pesaran [3] performed extensive bench scale experiments on thin beds of regular density silica gel with step changes in inlet air humidity. The data obtained reliably confirmed that the solid-side resistance was indeed generally larger than the gas-side resistance, and the need for a suitable model of intro-particle moisture transport was thus made clear. In this paper we present a model which accounts for both Knudsen diffusion and surface diffusion of moisture within the particle, and combine it with a model for the bed performance as a whole incorporating gas phase mass and heat transfer resistances. The solid-side heat transfer resistance is ignored since the characteristically small Biot number allows the assumption of negligible intra-particle temperature gradients. In Part II of this series, an associated experimental program is described, and comparisons made between model predictions and experimental data.

2. PREVIOUS WORK

The most pertinent study of moisture transport in silica gel particles is that of Kruckels [4], who performed both experimental and theoretical studies of water vapor adsorption by single isothermal silica gel particles: the experiments were performed with pure vapor to eliminate any gas-side resistance. The only resistance to mass transfer in the model was assumed to be surface diffusion in the pores. By comparing theoretical and experimental adsorption rates he concluded that the effective diffusivity inside the particles was a function of temperature, concentration and concentration gradient.

It was, however, relevant to also review the literature on other adsorbate–adsorbent systems in order to identify promising approaches to modeling moisture transport in silica gel. The work of Rosen [5] is often quoted: he assumed isothermal spherical particles with a homogeneous and isotropic pore system. A linear equilibrium relation was applied at the surface of the particle. The adsorbate was assumed to move through the pores by surface diffusion, or a mechanism similar to solid-phase diffusion, with a constant diffusion coefficient. Neretnieks [6] modeled isother-

† Present address: Solar Energy Research Institute, Golden, CO 80401, U.S.A.

NOMENCLATURE

a	average pore radius
A	cross-sectional area of bed
Bi_m	mass transfer Biot number, $K_G R/\rho_p D$
c	specific heat
c_l	specific heat of liquid water
$c_{p,e}$	constant pressure specific heat of humid air
c_{pl}	constant pressure specific heat of water vapor
DAR	desiccant to air ratio, $\rho_b AL/\dot{m}_G\tau$ [dimensionless]
D	total diffusivity, defined by equation (11)
D^*	$D\tau/R^2$ [dimensionless]
D_K	Knudsen diffusion coefficient
D_S	surface diffusion coefficient
Fo_m	mass transfer Fourier number, Dt/R^2
G_a	air mass flow rate per unit area
g	equilibrium isotherm, $\rho m = g(W, T)$
$g'(W)$	derivative of equilibrium isotherm, $\rho(\partial m_1/\partial W)_T$
h	enthalpy
h_l	enthalpy of water vapor
h_c	convective heat transfer coefficient
H_{ads}	heat of adsorption
ID	intermediate density (macroporous)
k	thermal conductivity
K_G	gas-side mass transfer coefficient
$K_{G,eff}$	effective mass transfer coefficient
L	length of bed
m_1	water vapor mass fraction [kg water/kg humid air]
$\dot{m}_G$	mass flow rate of gas mixture
n	mass flux
N_{tu}	number of transfer units, $K_G pL/\dot{m}_G$ or $K_{G,eff}pL/\dot{m}_G$ [dimensionless]
P	pressure
PGC	pseudo-gas-side controlled
p	perimeter of bed
r	radial coordinate in a particle
R	particle radius
R	H_2O gas constant
Re	Reynolds number, $2RV/v$ [dimensionless]
RD	regular density (microporous)
RH	relative humidity, P_1/P_{sat} [dimensionless]
S_g	specific pore surface area
SSR	solid-side resistance
t	time
t^*	dimensionless time, t/τ [dimensionless]
T	temperature [°C]
V	superficial velocity of air, G_a/ρ
W	desiccant water content [kg water/kg dry desiccant]
z	axial distance
z^*	z/L [dimensionless].

Greek symbols

β	$\rho_p D/K_G R$ [dimensionless]
ε	porosity [dimensionless]
v	kinematic viscosity
ρ	density of humid air
ρ_p	particle density
τ	duration of experimental run
τ_g	tortuosity factor for intraparticle gas diffusion [dimensionless]
τ_S	tortuosity factor for intraparticle surface diffusion [dimensionless].

Subscripts

0	initial value
1	water vapor
2	dry air
avg	average value
b	bed; bulk
e	surrounding humid air
eff	effective value
K	Knudsen diffusion
in	inlet value
out	outlet value
p	particle
S	surface diffusion
s	s-surface, in gas phase adjacent to gel particles, or dry solid phase of the bed
sat	saturation
u	u-surface, in solid phase adjacent to gel particles.

mal countercurrent adsorption by a fixed packed bed. Transport in the spherical particles was assumed to be by pore diffusion, solid diffusion, or a combination of both, with constant diffusion coefficients. The effect of the gas-side resistance was included. The model equations were solved numerically by use of the method of orthogonal collocation, and breakthrough curves were obtained. Schneider and Smith [7] investigated the significance of surface diffusion using the chromatographic method. The differential equations describing the concentration of an adsorbate flowing through a column containing spherical adsorbent particles were solved by the method of moments of the chromatographic curve. Both Knudsen and surface diffusion were considered as possible solid-side diffusion mechanisms, with constant diffusion

coefficients. Isothermal particles were assumed with a linear adsorption isotherm applied locally within the particles. Experimental data for adsorption of ethane, propane and n-butane on silica gel were used to determine surface diffusion coefficients.

Carter [8] modeled transient heat and mass transfer in an adiabatic fixed bed for situations where the heat of adsorption is significant. For mass transfer both a gas-side resistance and a solid-side resistance were included, while for heat transfer only a gas-side resistance was included. A constant solid-side diffusion coefficient was assumed and equilibrium was applied locally within the particle. Numerical solutions were obtained for adsorption of water vapor on activated alumina, and compared with experimental data from a full scale plant. Reasonable agreement was obtained and discrepancies were attributed to inaccurate equilibrium isotherms and surface diffusion coefficient inputs. Meyer and Weber [9] studied the adsorption of methane from helium carrier gas by beds of activated carbon particles, both experimentally and theoretically. Their model includes both gas-side and solid-side (Knudsen diffusion) resistances for mass transfer, and gas-side and solid-side (conduction) resistances for heat transfer. A general equilibrium adsorption relation was applied within a spherical particle. A constant Knudsen diffusion coefficient was used. Discrepancies between predictions and experiment were attributed to inaccuracies in experimentally determined diffusion coefficients for methane in activated carbon.

3. MODELING OF INTRA-PARTICLE MOISTURE TRANSPORT

Water vapor can diffuse through a porous medium by ordinary, Knudsen and surface diffusion. For silica gel at atmospheric pressure, the contribution by ordinary (Fick's law) diffusion is shown in Appendix A to be negligible, and only the latter two mechanisms of diffusion need to be considered. An equation describing conservation of moisture in a single spherical particle is developed here for the cases where either or both of the two diffusion mechanisms are important. The diffusion rates for each mechanism are compared for both regular density (RD) and intermediate density (ID) silica gel particles. RD gel has a microporous structure with an average pore radius of 11 Å while ID gel is a macroporous material and has an average pore radius of 68 Å. (Note that the H—O bond length in a water vapor molecule is 0.958 Å with a bond angle of 104.45° [10] and the distance between the two H atoms is 1.515 Å.)

Consider a spherical particle of silica gel (Fig. 1) with initial gel water content $W_0 = f(r)$, and a uniform temperature T_0, which is suddenly exposed to humid air with water vapor mass fraction $m_{1,e} = f(t)$. Assuming low mass transfer rates, water vapor is transferred from the bulk air stream to the particle surface at a rate

$$n_{1,s} = K_G(m_{1,s} - m_{1,e}). \tag{1}$$

Water molecules are assumed to move through pores by both Knudsen and surface diffusion, while adsorption takes place on the pore walls. The adsorption–desorption process is assumed to be rapid with respect to diffusion, and thus the local vapor concentration ρm_1 and the local gel water content W are in equilibrium. The differential equation governing H_2O conservation is

$$\varepsilon_p \frac{\partial(\rho m_1)}{\partial t} + \rho_p \frac{\partial W}{\partial t} = -\frac{1}{r^2}\frac{\partial}{\partial r}(r^2 n_1) \tag{2}$$

where n_1 is the mass flux of H_2O through the porous particle and consists of Knudsen diffusion, surface diffusion, and convective contributions.

The rate of Knudsen diffusion through the particle is

$$n_{1,K} = -\rho D_{K,eff}\frac{\partial m_1}{\partial r}$$

and the rate of surface diffusion is

$$n_{1,S} = -\rho_p D_{S,eff}\frac{\partial W}{\partial r}.$$

The effective Knudsen diffusivity, $D_{K,eff}$, and the effective surface diffusivity, $D_{S,eff}$, are discussed in the Appendix. Since Knudsen and surface diffusion are parallel processes, they are additive if the interactions between them are ignored. Adding the contributions to the mass flux of H_2O

$$n_1 = -\rho_p D_{S,eff}\frac{\partial W}{\partial r} - \rho D_{K,eff}\frac{\partial m_1}{\partial r} + m_1 n_1$$

where the third term on the right-hand side is the convection of water vapor through the pores assuming that the air is stationary. If $m_1 \ll 1$, as is the case in the present study ($m_1 < 0.03$), convection can be ignored, and

$$n_1 = -\rho_p D_{S,eff}\frac{\partial W}{\partial r} - \rho D_{K,eff}\frac{\partial m_1}{\partial r}. \tag{3}$$

Substituting equation (3) in equation (2) yields the differential equation

$$\varepsilon_p \frac{\partial(\rho m_1)}{\partial t} + \rho_p \frac{\partial W}{\partial t} = \frac{1}{r^2}\frac{\partial}{\partial r}\left[r^2 D_{S,eff}\rho_p \frac{\partial W}{\partial r}\right] + \frac{1}{r^2}\frac{\partial}{\partial r}\left[r^2 D_{K,eff}\rho \frac{\partial m_1}{\partial r}\right] \tag{4}$$

which requires two initial conditions and two boundary conditions.

The initial conditions are

$$W(r, t = 0) = W_0(r); \quad \rho m_1(r, t = 0) = \rho m_{1\,0}(r) \tag{5a, b}$$

while the boundary conditions are

zero flux at the center

$$n_1|_{r=0} = 0 \tag{6}$$

species continuity at the surface

$$n_1|_{r=R} = K_G(m_{1,s} - m_{1,e}). \tag{7}$$

Also local equilibrium is assumed between vapor and absorbed phase, thus ρm_1 and W within the particle are related through the equilibrium condition

$$\rho m_1(r,t) = g[W(r,t), T]. \tag{8}$$

Finally, continuity of gas phase concentrations requires

$$m_1(r = R, t) = m_{1,s}(t). \tag{9}$$

By setting either $D_{S,eff}$ or $D_{K,eff}$ equal to zero the limit cases of dominant Knudsen diffusion or dominant surface diffusion can be obtained.

3.1. *Generalized diffusion equation*

The above equations can be simplified by assuming an isothermal particle, which is reasonable for this study since the Biot number of the silica gel particles is generally less than 0.15 [11]. The number of unknowns can be reduced by eliminating ρm_1 using the equilibrium relation, equation (8), and the chain rule of differentiation to obtain

$$\frac{\partial}{\partial t}(\rho m_1) = \left(\frac{\partial(\rho m_1)}{\partial W}\right)_T \frac{\partial W}{\partial t} = g'(W)\frac{\partial W}{\partial t}$$

$$\frac{\partial}{\partial r}(\rho m_1) = \left(\frac{\partial(\rho m_1)}{\partial W}\right)_T \frac{\partial W}{\partial r} = g'(W)\frac{\partial W}{\partial r}.$$

Since $m_1 \ll 1$, and the particle is taken to be isothermal, ρ can be assumed to be constant inside the particle; hence

$$\frac{\partial(\rho m_1)}{\partial r} \simeq \rho \frac{\partial m_1}{\partial r}.$$

Substituting the above equations into equation (4) and rearranging gives

$$\frac{\partial W}{\partial t} = \frac{1}{(\varepsilon_p g'(W)/\rho_p + 1)} \frac{1}{r^2}\frac{\partial}{\partial r}\left\{r^2\left[D_{S,eff} + D_{K,eff}\frac{g'(W)}{\rho_p}\right]\frac{\partial W}{\partial r}\right\}. \tag{10}$$

For both RD and ID gel $g'(W)$ varies from 0 to 0.4 kg m^{-3} [11], ε_p is less than unity and ρ_p is 1129 and 620 kg m^{-3} for RD and ID gel, respectively. Thus $\varepsilon_p g'(W)/\rho_p$ is at most of the order of 5×10^{-4}; it is negligible compared to unity and will be ignored. Physically this corresponds to neglecting the gas phase storage term $\varepsilon_p \partial(\rho m_1)/\partial t$ in equation (4). We now define a total diffusivity D

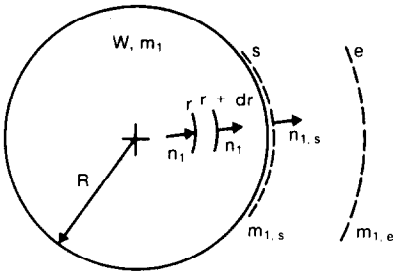

FIG. 1. Diffusion through a spherical particle.

$$D = D_{S,eff} + D_{K,eff}\frac{g'(W)}{\rho_p} \tag{11}$$

where D is a function of both gel water content W and particle temperature. Equations (5)–(10) then become

$$\frac{\partial W}{\partial t} = \frac{1}{r^2}\frac{\partial}{\partial r}\left[r^2 D \frac{\partial W}{\partial r}\right] \tag{12}$$

I.C. $$W(r, t = 0) = W_0(r) \tag{13}$$

B.C. 1 $$\left.\frac{\partial W}{\partial r}\right|_{r=0} = 0 \tag{14}$$

B.C. 2 $$-\rho_p D \left.\frac{\partial W}{\partial r}\right|_{r=R} = K_G(m_{1,s} - m_{1,e}) \tag{15}$$

Coupling (or equilibrium) condition:

$$m_{1,s}(t) = f[W(r = R, t), T, P]. \tag{16}$$

The above set of equations applies to any combination of Knudsen and surface diffusion. Equations (11)–(16) will be used in the analysis of silica gel bed performance presented later.

3.2. *Comparison of surface and Knudsen diffusion fluxes in a particle*

The ratio of Knudsen to surface diffusion fluxes in a gel particle is

$$\frac{n_{1,K}}{n_{1,S}} = \frac{D_{K,eff} g'(W)/\rho_p}{D_{S,eff}}. \tag{17}$$

If we substitute equations (A4) and (A8) we obtain

$$\frac{n_{1,K}}{n_{1,S}} = \frac{\tau_S \varepsilon_p}{\tau_g \rho_p}\frac{D_K}{D_S} g'(W).$$

This ratio depends on the internal structure of the particle (average pore radius, surface area, tortuosity factors), isotherm slope and temperature. The results of calculations for this ratio show [11] that the dominant mechanism in RD gel is surface diffusion,

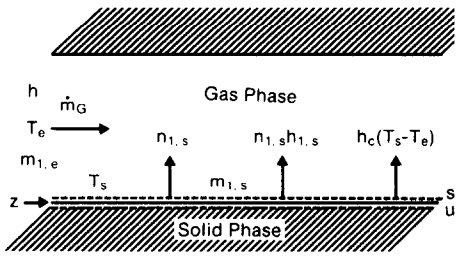

FIG. 2. Idealized picture of the physical phenomena in the gas phase of the packed bed.

while both surface and Knudsen diffusion should be considered for ID gel. This conclusion is consistent with the conclusion arrived at in the Appendix for a single pore. In fact, assuming the Wheeler [12] porous model of straight and cylindrical pores, it can be shown [11] that equations (17) and (A11) are identical.

4. MODELING OF SILICA GEL PACKED PARTICLE BEDS

The differential equations governing the transient response of a packed bed of desiccant particles are presented in this section. These equations are obtained by applying the principles of mass, species, and energy conservation in both solid and gas phases. Figure 2 shows an idealized picture of the physical phenomena in the gas phase. The species conservation equation in the gas phase neglecting axial and radial diffusion is

$$\varepsilon_b A\frac{\partial(\rho m_1)_e}{\partial t}+\frac{\partial(m_{1,e}\dot{m}_G)}{\partial z}=n_{1,s}p \tag{18}$$

while overall mass conservation requires that

$$\varepsilon_b A\frac{\partial\rho_e}{\partial t}+\frac{\partial\dot{m}_G}{\partial z}=n_{1,s}p. \tag{19}$$

Combining equations (18) and (19) gives

$$\varepsilon_b A\rho_e\frac{\partial m_{1,e}}{\partial t}+\dot{m}_G\frac{\partial m_{1,e}}{\partial z}=n_{1,s}(1-m_{1,e})p. \tag{20}$$

It can be shown [11] that the storage term $\varepsilon_b A\rho_e(\partial m_{1,e}/\partial t)$ is negligible for thin beds. Assuming low mass transfer rates the final form of equation (20) is

$$\dot{m}_G\frac{\partial m_{1,e}}{\partial z}=K_G(m_{1,s}-m_{1,e})(1-m_{1,e})p. \tag{21}$$

The species conservation equation for the solid phase was developed in Section 3. For spherical particles assuming radial symmetry the general form of the equation is equation (12)

$$\frac{\partial W}{\partial t}=\frac{1}{r^2}\frac{\partial}{\partial r}\left(Dr^2\frac{\partial W}{\partial r}\right) \tag{22a}$$

where D, the total diffusivity defined by equation (11), is a function of gel water content W. Note that if the mass transfer problem is treated as a 'lumped capacitance' model, as has been done by many investigators, e.g. refs. [1, 13, 14] in their pseudo-gas-side controlled models, the solid-phase species conservation equation becomes

$$A\rho_b\frac{\partial W_{avg}}{\partial t}=-K_{G,eff}(m_{1,s}-m_{1,e})p \tag{22b}$$

where $K_{G,eff}$ is an effective mass transfer coefficient, accounting for both gas-side and solid-side resistances. Equations (21) and (22a) are coupled through the equilibrium relation applied at the particle surface

$$m_{1,s}(z,t)=f[W(r=R,z,t),T_s(z,t),P]. \tag{23}$$

The initial and boundary conditions for equation (22a) are

I.C. $$W(r,z,t=0)=W_0 \tag{24}$$

B.C. 1 $$\left.\frac{\partial W}{\partial r}\right|_{r=0}=0 \tag{25}$$

B.C. 2 $$-\rho_p D\left.\frac{\partial W}{\partial r}\right|_{r=R}=K_G[m_{1,s}(z,t)-m_{1,e}(z,t)] \tag{26}$$

while the boundary condition for equation (21) is

$$m_{1,e}(z=0,t)=m_{1,in}. \tag{27}$$

The average water content of a particle is given by

$$W_{avg}=\frac{\int_0^R 4\pi r^2 W\rho_p\,dr}{(4/3)\pi R^3\rho_p}. \tag{28}$$

Referring to Fig. 2, the gas-phase energy conservation equation is

$$\frac{\partial}{\partial z}(\dot{m}_G h)=p[h_c(T_s-T_e)+n_{1,s}h_{1,s}] \tag{29}$$

where axial and radial conduction and the storage term have been neglected and the bed is assumed to be adiabatic. Assuming isothermal particles a 'lumped capacitance' model can be used for the solid phase. Then energy conservation in the solid phase is

$$A\rho_b\frac{\partial h_b}{\partial t}=-p[h_c(T_s-T_e)+n_{1,s}h_{1,s}]. \tag{30}$$

Assuming low mass transfer rates and using

$$h_b=\int_0^W h_{1,u}\,dW'+h_{solid}$$

$$H_{ads}(W_{avg})=h_{1,s}-h_{1,u}$$

$$c_b(W_{avg})=W_{avg}c_1+c_{solid}$$

$$h=m_1h_1+(1-m_1)h_2$$

$$c=\frac{\partial h}{\partial T}$$

equations (29) and (30) can be rewritten in terms of temperatures as

$$c_{p,e}\dot{m}_G\frac{\partial T_e}{\partial z} = -p[h_c + c_{p1}K_G(m_{1,s} - m_{1,e})] \times (T_e - T_s) \quad (31)$$

$$A\rho_b c_b\frac{\partial T_s}{\partial t} = p[h_c(T_e - T_s) - H_{ads}K_G(m_{1,s} - m_{1,e})]. \quad (32)$$

The initial condition for equation (32) is

$$T_s(z, t = 0) = T_0 \quad (33)$$

while the boundary condition for equation (31) is

$$T_e(z = 0, t) = T_{in}. \quad (34)$$

Equations (21), (22a), (23), (28), (31) and (32) are a set of coupled non-linear equations with six unknowns: $W(r, z, t)$, $W_{avg}(z, t)$, $m_{1,s}(z, t)$, $T_s(z, t)$, $m_{1,e}(z, t)$ and $T_e(z, t)$. These can be solved with the given boundary and initial conditions.

4.1. *Auxiliary data*

Data are required for K_G, h_c, D, $c_{p,e}$, c_b, H_{ads} and the equilibrium relation. Based on a survey of the available literature on mass transfer in packed particle beds [3] the following correlations for the gas-side transfer coefficients are adopted

$$K_G = 1.70G_a Re^{-0.42}\,\mathrm{kg\,m^{-2}\,s^{-1}} \quad (35)$$

$$h_c = 1.60G_a Re^{-0.42}c_{p,e}\,\mathrm{W\,m^{-2}\,K^{-1}}. \quad (36)$$

For the pseudo-gas-side controlled model $K_{G,eff}$ and h_c are given by the Hougen and Marshall correlations [15] of Ahlberg's experimental data [16] since these are in wide use

$$K_{G,eff} = 0.704G_a Re^{-0.51}\,\mathrm{kg\,m^{-2}\,s^{-1}} \quad (37)$$

$$h_c = 0.683G_a Re^{-0.51}c_{p,e}\,\mathrm{W\,m^{-2}\,K^{-1}}. \quad (38)$$

The total diffusivity can be obtained using equation (11) and the expressions given in the Appendix. The specific heats $c_{p,e}$ and c_b are given by

$$c_{p,e} = 1884m_{1,e} + 1004(1 - m_{1,e})\,\mathrm{J\,kg^{-1}\,K^{-1}} \quad (39)$$

$$c_b = 4186W_{avg} + 921\,\mathrm{J\,kg^{-1}\,K^{-1}}. \quad (40)$$

Equilibrium isotherms were obtained by fitting fourth-degree polynomials to the manufacturer's data [11] for regular density (Davison, Grade 01) and intermediate density (Davison, Grade 59):

for RD gel

$$\mathrm{RH} = 0.0078 - 0.05759W + 24.16554W^2 - 124.478W^3 + 204.226W^4 \quad (41)$$

for ID gel

$$\mathrm{RH} = 1.235W + 267.99W^2 - 3170.7W^3 + 10087.16W^4, \quad W \leqslant 0.07$$
$$\mathrm{RH} = 0.3316 + 3.18W, \quad W > 0.07. \quad (42)$$

The relation between water vapor mass fraction and relative humidity, RH, is

$$m_1 = \frac{0.622\mathrm{RH} \times P_{sat}(T)}{P_{total} - 0.378\mathrm{RH} \times P_{sat}(T)}.$$

The heat of adsorption for RD gel is

$$\left.\begin{aligned} H_{ads} &= -12400W + 3500, W \leqslant 0.05 \\ H_{ads} &= -1400W + 2950, \ W > 0.05 \end{aligned}\right\}\ \mathrm{kJ/kg\ water} \quad (43)$$

and for ID gel is

$$\left.\begin{aligned} H_{ads} &= -300W + 2095, W \leqslant 0.15 \\ H_{ads} &= 2050, \qquad\quad W > 0.15 \end{aligned}\right\}\ \mathrm{kJ/kg\ water.} \quad (44)$$

4.2. *Method of solution*

The above set of equations was put in dimensionless form and solved numerically. Three non-dimensional parameters were involved

$$N_{tu} = \frac{K_G pL}{\dot{m}_G}; \qquad \mathrm{DAR} = \frac{\rho_b AL}{\dot{m}_G\tau}; \qquad \beta = \frac{\rho_p D}{K_G R}.$$

The Crank–Nicholson scheme was used for equation (22a), while the implicit Euler method was used for equations (32) and (22b). A fourth-order Runge–Kutta technique was used for the spatial equations, equations (21) and (31). For further details of the numerical procedure see ref. [11]. A computer code called DESICCANT was developed which is capable of producing numerical solution to the following transient problems.

(1) Step change in surrounding water vapor concentration of a single isothermal silica gel particle (equation (22a)).

(2) Step change in the inlet conditions to a fixed packed bed of silica gel with solid-side resistance (SSR) model (equations (21), (22a), (23), (28), (31) and (32)).

(3) Step change in the inlet conditions to a fixed packed bed of silica gel with pseudo-gas-side controlled (PGC) model (equations (21), (22b), (23), (31) and (32)). Note that for this case $N_{tu} = K_{G,eff}pL/\dot{m}_G$.

5. RESULTS AND DISCUSSIONS

The numerical solutions of the diffusion equation for a single particle, equation (12), for RD and ID silica gels are discussed first. Next, the bed performance using the theoretical models, i.e. SSR and PGC models, will be presented for RD and ID silica gels for both adsorption and desorption cases. Note that the major difference between these two

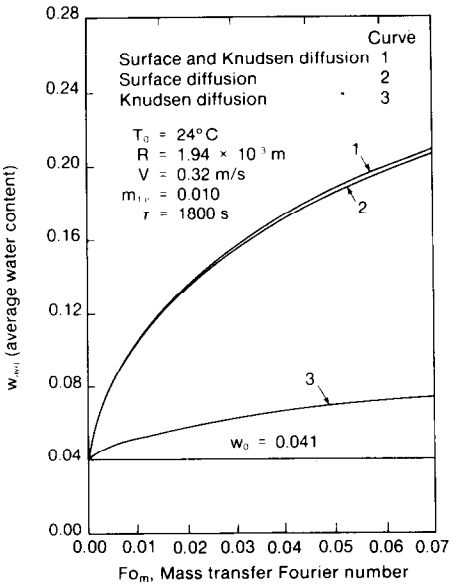

FIG. 3. W_{avg} vs mass transfer Fourier number for various mechanisms of diffusion for an RD particle.

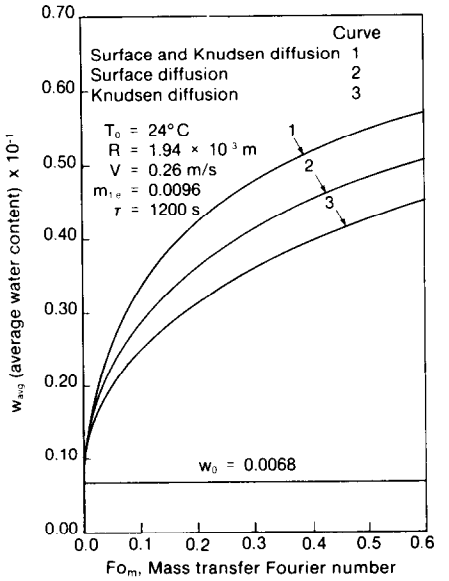

FIG. 4. W_{avg} vs mass transfer Fourier number for various mechanisms of diffusion for an ID particle.

models is the use of the diffusion equation, equation (22a), in the SSR model and use of the 'lumped capacitance' equation, equation (22b), in the PGC model. The SSR model includes both gas-side and diffusion resistances inside the particles; the PGC model is a lumped capacitance model. Adsorption occurs when the bed is initially dry relative to the inlet air, and moisture is transferred to the silica gel. Desorption occurs when the inlet air is dry relative to the initial condition of the bed, and moisture is transferred from the silica gel particles.

5.1. *Numerical solutions of the diffusion equation in an isothermal particle*

The numerical solutions to the diffusion equation for an RD and an ID particle are presented in Figs. 3 and 4, respectively. The particle has an initial water content of W_0, and at $t = 0$ there is a step change in the water vapor mass fraction of the surroundings to $m_{1,e}$. The figures show the gel water content as a function of mass transfer Fourier number for adsorption cases. The Fourier number was estimated based on initial D. The result for an RD particle, Fig. 3, shows that the difference between curve 1 (surface plus Knudsen diffusion) and curve 2 (surface diffusion only) is very small, and thus confirm that the contribution of Knudsen diffusion can be neglected for RD gel. On the other hand, Fig. 4 shows that the contribution of Knudsen diffusion cannot be neglected for ID gel. Note that the curves of W_{avg} vs Fo_m for each mechanism cannot be simply added, since the problem is a nonlinear one. It should be noted that the same value of $D_{0,eff}$ ($= 1.6 \times 10^{-6}$) for both ID and RD gel was used to estimate surface diffusivity from equation (A8). This value of $D_{0,eff}$ was obtained as a best estimate through comparison of experimental

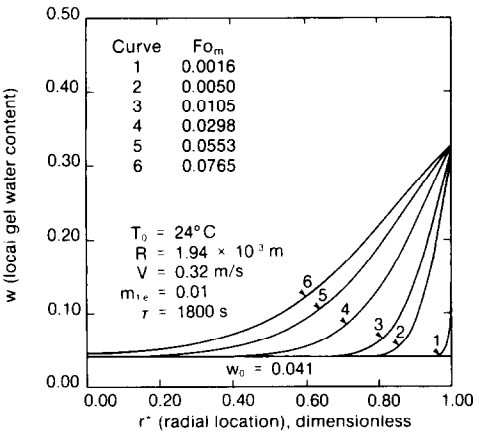

FIG. 5. Concentration profile in an RD particle with surface diffusion.

and theoretical results, as explained in refs. [11,21]. The results shown in Figs. 3 and 4 are general over a wide range of temperature ($20 < T < 50$°C) and humidity (<0.03 kg/kg humid air).

The local concentration profiles in RD and ID particles at different times are plotted in Figs. 5 and 6, respectively. It is observed that usually the gel water content at the surface reaches about 90% of its final equilibrium value when t^* reaches 0.1–0.15. The shape of the profiles in both gels are the same. However, the penetration of water into ID gel is faster than that of RD gel mainly because the total diffusivity, D, of ID gel is much larger than that of RD gel (about 4–20 times greater).

5.2. *Numerical solutions for bed performance using SSR and PGC models*

The range of parameters (i.e. initial bed conditions, air velocity, inlet air conditions, etc.) which were used to generate the numerical solutions in this section are

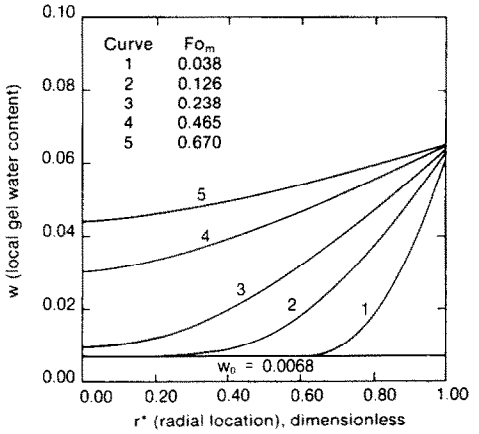

FIG. 6. Concentration profile in an ID particle with surface and Knudsen diffusions.

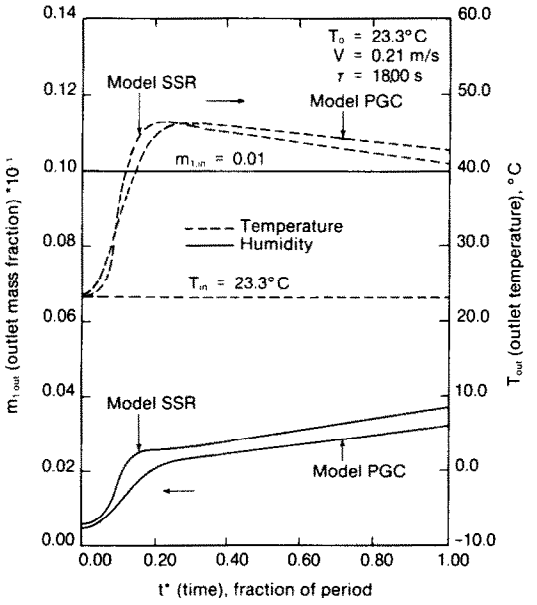

FIG. 7. Comparison of PGC and SSR models for adsorption on RD gel, Run 1.

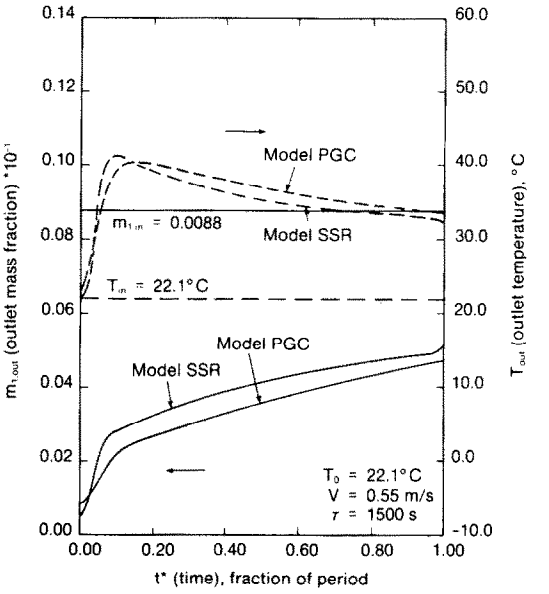

FIG. 8. Comparison of PGC and SSR models for adsorption on RD gel, Run 2.

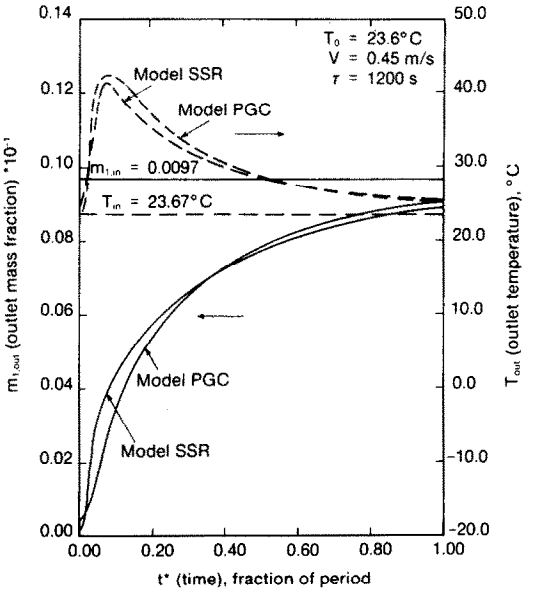

FIG. 9. Comparison of PGC and SSR models for adsorption on ID gel, Run 3.

typical of those that are encountered in the operation of solar desiccant cooling systems. The numerical solutions were obtained for a bed of initially uniform conditions (W_0, T_0) with a step change in the inlet air conditions (T_{in}, $m_{1,in}$) at time $t = 0$. It should be noted that, hereafter, whenever the SSR model is used for RD gel only surface diffusion is considered in the particles while for ID gel both surface and Knudsen diffusions are included in the SSR model.

Typical theoretical results using both the model with solid-side resistance (SSR model) and pseudo-gas-side controlled model (PGC model) are presented in Figs. 7–12. Table 1 summarizes the pertinent parameters. The mass transfer Biot number, Bi_m, in Table 1 indicates the relative importance of the solid-side and gas-side mass transfer resistances. The lower Biot number for ID gel is mainly due to higher total diffusivity D in the particles. Note that the dimensionless parameter β is the reciprocal of Bi_m. In the figures, the outlet air temperature (T_{out}) and water vapor mass fraction ($m_{1,out}$) after the step change in the inlet conditions to the bed, are shown as a function of dimensionless time t/τ. Duration of an experiment, τ, is about half of the cycle time for fixed silica gel beds and τ has a fundamental relevance for making time dimensionless. Since both gas- and solid-side resistances are considered here, the Fourier number is not an appropriate time scale. Figures 7 and 8 are typical results for adsorption on RD silica gel beds,

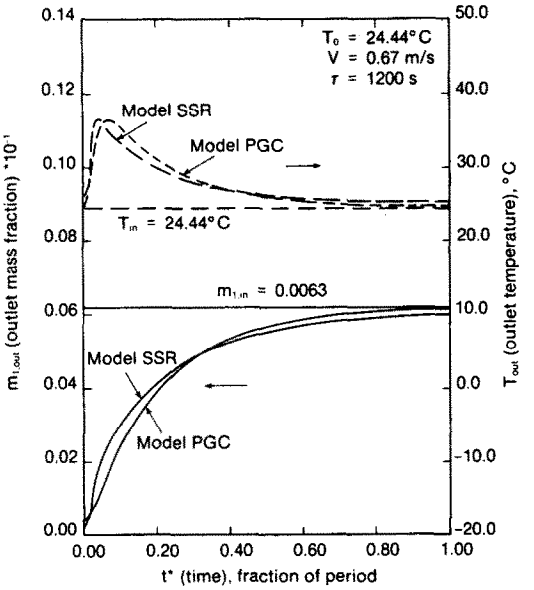

FIG. 10. Comparison of PGC and SSR models for adsorption on ID gel, Run 4.

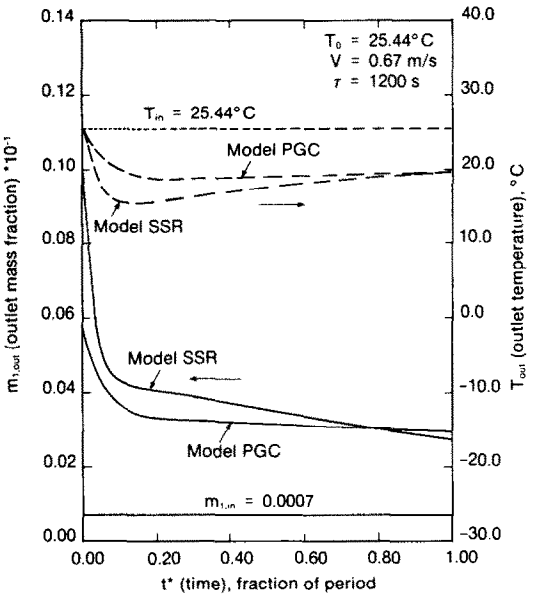

FIG. 12. Comparison of PGC and SSR models for desorption on RD gel, Run 6.

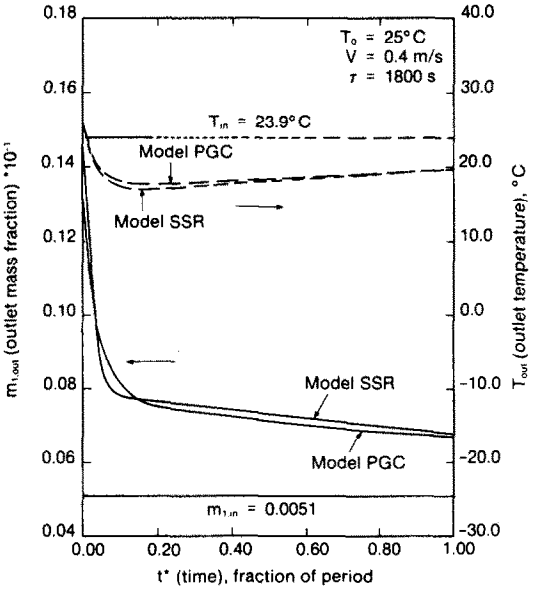

FIG. 11. Comparison of PGC and SSR models for desorption on RD gel, Run 5.

Figs. 9 and 10 are typical results for adsorption on ID silica gel, and results for desorption from RD silica gel are presented in Figs. 11 and 12. Theoretical predictions of the SSR model in these figures were obtained using $D_{s,eff}$ from equation (A8) with $D_{0,eff} = 1.6 \times 10^{-6}$.

The general trend of the predicted results from both models for adsorption cases can be explained as follows: T_{out} increases rapidly to a maximum and gradually decreases at a rate depending on the air flow rate; $m_{1,out}$ also increases rapidly at first, but rather than reaching a maximum, the rate of increase simply becomes less. The change in slope of $m_{1,out}$ occurs after T_{out} reaches its peak. The reasons for this behavior can be explained as follows. Immediately following the step change, the dry bed adsorbs H_2O and liberates heat at a high rate; consequently the bed temperature and T_{out} increases rapidly, and $m_{1,out}$ increases rapidly from a value much lower than $m_{1,in}$. The bed gradually loses its adsorptive capacity due to the increase in gel water content and bed temperature, and the rate of increase of $m_{1,out}$ decreases as a result. The maximum in T_{out} is reached when the cooling effect of the air flow balances the heat of adsorption being released, and thereafter the reduced rate of adsorption causes T_{out} to decrease. The reverse of the above explanation is valid for the desorption cases.

Generally the initial rates of increase of $m_{1,out}$ predicted by the SSR model are steeper than those predicted by the PGC model. This feature can be explained as follows. The PGC model has a constant overall mass transfer resistance chosen to best approximate the adsorption process on an average basis. The SSR model has an overall resistance which increases as the adsorption process proceeds and moisture has to diffuse further into the gel particle. Thus, initially, the overall resistance of the SSR model is lower than that of the PGC model, adsorption rates are higher, and the outlet concentration predicted by the SSR model increases faster than that predicted by the PGC model. During the latter stages of adsorption the situation is reversed so that the total amount of water adsorbed would be the same for both models.

In general the shape of the $m_{1,out}$ and T_{out} curves predicted by the SSR model are not the same for adsorption vs desorption. This interesting feature is

Table 1. Bed and flow conditions for the theoretical solutions

Run	Gel	Process	R ($m \times 10^{-3}$)	L ($m \times 10^{-3}$)	W_0 (kg/kg)	T_0 (°C)	T_{in} (°C)	$m_{1,in}$	V ($m\,s^{-1}$)	τ (s)	N_{tu}†	Bi_m‡	DAR
1	RD	Adsorption	1.94	77.5	0.0417	23.3	23.3	0.0100	0.21	1800	22.65	1145	0.1285
2	RD	Adsorption	1.94	75.0	0.045	22.1	22.1	0.0088	0.55	1500	14.25	2401	0.0547
3	ID	Adsorption	1.94	77.5	0.0088	23.6	23.7	0.0097	0.45	1200	16.85	175	0.0500
4	ID	Adsorption	1.94	77.5	0.005	24.4	24.5	0.0063	0.67	1200	14.21	222	0.0330
5	RD	Desorption	2.60	50.0	0.368	25.0	25.0	0.0051	0.40	1800	7.59	342	0.0420
6	RD	Desorption	2.60	50.0	0.260	25.4	25.4	0.0007	0.67	1200	6.12	723	0.0390

† This value of N_{tu} is for the SSR model, N_{tu} for the PGC model is about 1/3.4 of this value.
‡ Based on the initial value of D.

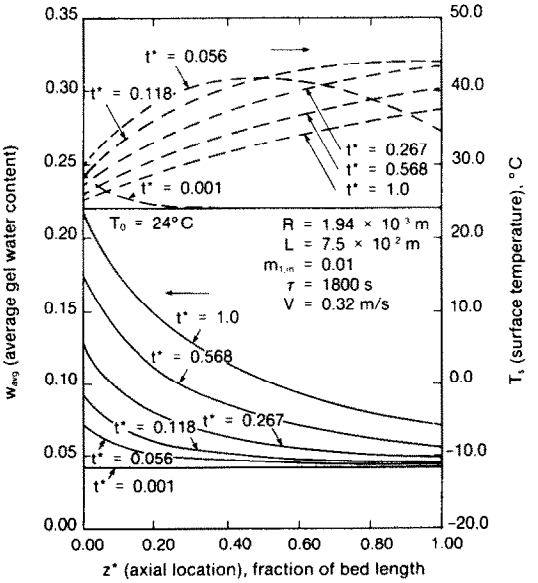

FIG. 13. Variation of W_{avg} and T_s with z^* at various t^* using the SSR model for adsorption on RD gel.

due to the concentration dependence of the surface diffusion coefficient, and the fact that the initial gel water content for a typical desorption case is much higher than for an adsorption case. Sladek's equation, equation (A7), shows that D_S increases with W. Hence, for all other pertinent parameters the same, the SSR model predicts a higher initial rate of desorption than adsorption. The PGC model does not have this feature.

The equilibrium capacity of ID gel is lower than RD gel, as one can calculate from equations (41) and (42). Thus, a bed of ID gel loses its adsorption capacity faster than a bed of RD gel with similar bed and air inlet conditions. This can be observed from comparison of numerical solutions from RD gel (Figs. 7 and 8) and ID gel (Figs. 9 and 10). The numerical predictions will be compared with the experimental results in Part II of this study [21] to evaluate the suitability of the models.

Figure 13 shows the variation of average gel water content and bed temperature along the bed at various times of a typical adsorption case on RD gel using the SSR model. Along the bed W_{avg} decreases monotonically, but the variation of T_s is more complex, associated with movement of the location of maximum adsorption rate along the bed with time.

6. SUMMARY AND CONCLUSIONS

The magnitude of different diffusion mechanisms into two types of silica gel particles was examined. It was found that in ID silica gel with a mean pore radius of 68 Å, both surface and Knudsen diffusion are important modes of moisture transport, while in RD silica gel with a mean pore radius of 11 Å, only surface diffusion needs to be considered. A generalized diffusion equation was developed and was incorporated in a simultaneous heat and mass transfer model to predict the transient performance of a packed bed of silica gel. The heat and mass transfer model was solved numerically using finite difference methods. The transient responses of silica gel beds to step change in inlet air conditions were predicted with this new model and were compared with the predictions of the widely used pseudo-gas-side controlled model. The new model is more faithful to the true physics of the problem, so it is likely that it will give better agreement with experimental results. Comparison with experiment will be reported in Part II of this series [21].

Acknowledgments—This work was supported by a grant from the Solar Energy Research Institute/U.S. Department of Energy, Grant No. DE-FG02-80CS84056. The Technical Monitor was T. Penney. Computer time was supplied by the Campus Computing Network of the University of California, Los Angeles. The Publication Development Branch of the Solar Energy Research Institute assisted in preparing this paper.

REFERENCES

1. C. E. Bullock and J. L. Threlkeld, Dehumidification of moist air by adiabatic adsorption, *Trans. ASHRAE* **72**, part I, 301–313 (1966).
2. J. E. Clark, A. F. Mills and H. Buchberg, Design and testing of thin adiabatic desiccant beds for solar air conditioning applications, *J. Solar Energy Engng* **103**, 89–91 (May 1981).
3. A. A. Pesaran, Air dehumidification in packed silica gel beds, M.S. Thesis, School of Engineering and Applied Science, University of California, Los Angeles (1980).
4. W. W. Kruckels, On gradient dependent diffusivity,

Chem. Engng Sci. **28**, 1565–1576 (1973).
5. J. B. Rosen, Kinetics of a fixed bed system for solid diffusion into spherical particles, *J. chem. Phys.* **20**, 387–393 (1952).
6. I. Neretnieks, Adsorption in finite bath and counter-current flow with systems having a nonlinear isotherm, *Chem. Engng Sci.* **31**, 107–114 (1976).
7. P. Schneider and J. M. Smith, Chromatographic study of surface diffusion, *A.I.Ch.E.Jl* **14**(6), 886–895 (November 1968).
8. J. W. Carter, A numerical method for prediction of adiabatic adsorption in fixed beds, *Trans. Instn chem. Engrs* **44**, T253–T259 (1966).
9. O. A. Meyer and T. W. Weber, Nonisothermal adsorption in fixed beds, *A.I.Ch.E.Jl* **13**(3), 457–465 (1967).
10. R. C. Weast, *CRC Handbook of Chemistry and Physics*, p. F-168. CRC Press, Florida (1985).
11. A. A. Pesaran, Moisture transport in silica gel particle beds, Ph.D. Dissertation, School of Engineering and Applied Sciences, University of California, Los Angeles (1983).
12. A. Wheeler, Reaction rates and selectivity. In *Catalysis, II* (Edited by P. H. Emmett), pp. 109–120. Reinhold, New York (1955).
13. J. W. Nienberg, Modeling of desiccant performance for solar-desiccant-evaporative cooling systems, M.S. Thesis, School of Engineering and Applied Science, University of California, Los Angeles (1977).
14. F. E. Pla-Barby and G. C. Vliet, Rotary bed solid desiccant drying: an analytical and experimental investigation, *ASME/AIChE 18th National Heat Transfer Conference*, San Diego, California (1979) (ASME paper 79-HT-19).
15. O. A. Hougen and W. R. Marshall, Jr., Adsorption from a fluid stream flowing through a stationary granular bed, *Chem. Engng Prog.* **43**(4), 197–208 (April 1947).
16. J. E. Ahlberg, Rates of water vapor adsorption for air by silica gel, *Ind. Engng Chem.* **31**, 988–992 (August 1939).
17. D. K. Edwards, V. E. Denny and A. F. Mills, *Transfer Processes*, 2nd edn. Hemisphere/McGraw-Hill, New York (1979).
18. E. A. Flood, R. H. Tomlinson and A. E. Legger, The flow of fluids through activated carbon rods, *Can. J. chem. Engng* **30**, 389–396 (1952).
19. E. R. Gilliland, R. F. Baddour and J. L. Russel, Rates of flow through microporous solids, *A.I.Ch.E.Jl* **4**(1), 90–96 (March 1958).
20. K. J. Sladek, E. R. Gilliland and R. F. Baddour, Diffusion on surfaces. II. Correlation of diffusivities of physically and chemically adsorbed species, *Ind. Engng Chem. Fundam.* **13**(2), 100–105 (1974).
21. A. A. Pesaran and A. F. Mills, Moisture transport in silica gel particle beds—II. Experimental study, *Int. J. Heat Mass Transfer* **30**, 1051–1060 (1987).

APPENDIX. DIFFUSION IN POROUS MEDIA

Ordinary diffusion, as described by Fick's law, occurs when the molecules of the gas collide with each other more frequently than with pore walls of a porous medium. For water vapor–air mixtures a useful formula for the ordinary diffusion coefficient is [17]

$$D_{H_2O,air} = 1.735 \times 10^{-9} \times \frac{(T + 273.15)^{1.685}}{P} \text{ m}^2\text{s}^{-1} \quad \text{(A1)}$$

where T is the gas temperature in degrees Celsius and P is in atmospheres.

In the limit of large Knudsen number ($Kn = \lambda/a$, where λ is the mean free path and a is the pore radius) the gas molecules collide more often with pore walls than with each other and the diffusion of molecules is described by the equations of free molecule flow [18]. A Fick's law type expression can be obtained for this type of flow if a Knudsen diffusion coefficient, D_K, is defined. For water–vapor diffusion in straight cylindrical pores of radius a, a dimensional equation for D_K is [17]

$$D_K = 22.86a(T + 273.15)^{1/2} \text{ m}^2\text{s}^{-1} \quad \text{(A2)}$$

where a is in meters. Table A1 compares Knudsen and ordinary diffusion coefficients in water vapor–air mixtures for various values of pore radius. Note that combined ordinary and Knudsen diffusion may be approximately represented by assuming additive resistances [17], that is

$$\frac{1}{D_1} = \frac{1}{D_{H_2O,air}} + \frac{1}{D_K}. \quad \text{(A3)}$$

We see in Table A1 that Knudsen diffusion is dominant for pore sizes smaller than about 200 Å. Since most of the pores of silica gel are less than 100 Å, it is clear that ordinary diffusion can be ignored in usual silica gel applications.

Table A1. Comparison of Knudsen and ordinary diffusion coefficients in water vapor–air mixtures for various values of pore radius ($T = 40°C$, $P = 1$ atm)

a (Å)	D_{K,H_2O} ($m^2 s^{-1}$)	$D_{H_2O,air}$ ($m^2 s^{-1}$)	$\frac{D_{K,H_2O}}{D_{H_2O,air}}$
11	4.45×10^{-7}	2.79×10^{-5}	0.0159
68	2.75×10^{-6}	2.79×10^{-5}	0.099
100	4.04×10^{-6}	2.79×10^{-5}	0.145
200	8.08×10^{-6}	2.79×10^{-5}	0.290
1000	4.04×10^{-5}	2.79×10^{-5}	1.450

Equation (A2) is, strictly speaking, valid only for long, uniform radius capillaries, and should be modified for application to real porous media. It can be shown that [11] the effective Knudsen diffusion coefficient is related to Knudsen diffusion by

$$D_{K,eff} = \frac{\varepsilon_p}{\tau_g} D_K \quad \text{(A4)}$$

where ε_p is the particle porosity (volume void fraction) which accounts for the reduction of free area for diffusion due to the presence of solid phase and τ_g in the gas tortuosity factor which accounts for the increase in diffusional length due to tortuous paths of real pores. Note that the effective ordinary diffusion can also be obtained by an equation similar to equation (A4).

Surface diffusion is the transport of adsorbed molecules on the pore surface. A number of possible mechanisms for movement of adsorbed molecules on surfaces is proposed, e.g. refs. [4, 18, 19]. Kruckels [4] studied the surface diffusion of water vapor through isothermal RD silica gel particles. He expressed the surface rate in terms of Fick's law and considered the submonolayer concentration range (concentrations up to about half of the saturation loading of silica gel particles), and proposed that the mechanism of surface diffusion to be one of activated hopping molecules in a random walk process. He proposed a formula with several parameters: but since the theoretical estimation of these parameters was difficult, they were calculated by a non-linear least squares fit between the mathematical model and experimental data at 40°C. The resulting formula for the surface diffusion coefficient can be extrapolated to other

temperatures using the assumption of Arrhenius type behavior

$$D_S = 1.287 \times 10^{-8} \exp\left[-811.30\frac{W}{(T+273.15)}\right] \times \left[1 + 3112W\frac{\tanh(0.265 \times 10^{-2}(\partial W/\partial r))}{(\partial W/\partial r)}\right] m^2 s^{-1} \quad (A5)$$

and shows a decrease of D_S with increasing W.

This formula requires considerable computational effort, and is only valid for RD gels at low concentrations. A simpler formula which can be used for both RD and ID silica gel at both high and low concentrations was therefore sought.

Sladek *et al.* [20] proposed a simpler formula which is valid for both low and high surface coverages. They assumed a mechanistic hopping model with the assumption that the jumping frequency is a function of surface concentration (through the heat of adsorption) and obtained the following expression for the surface diffusion coefficient

$$D_S = D_0 \exp[-aH_{ads}/R(T+273.15)]. \quad (A6)$$

They later correlated some available data on surface diffusion of various adsorbates into different adsorbents (not H_2O–silica gel system) with this equation and found that D_0 should be set at $1.6 \times 10^{-6} m^2 s^{-1}$ and $a = 0.45/b$ where b is obtained from the type of adsorption bond. For silica gel, b is unity so the surface diffusivity becomes

$$D_S = D_0 \exp[-0.974 \times 10^{-3} \times (H_{ads}/(T+273.15))] m^2 s^{-1} \quad (A7)$$

where an approximation to D_0 is $1.6 \times 10^{-6} m^2 s^{-1}$. However, as we will see in Part II of this study, D_0 can be obtained by matching the experimental and theoretical results of the transient response of packed beds of silica gel.

The surface diffusion coefficients given above are valid for smooth surfaces, and should be modified to account for the rough walls of the porous media. Since surface diffusion is a surface phenomenon the reduction of the area normal to the direction of flux due to the presence of the solid phase has no role in effective surface diffusivity.

It can be shown [11] that

$$D_{S,eff} = \frac{1}{\tau_s} D_S = D_{0,eff} \exp[-0.947 \times 10^{-3}(H_{ads}/(T+273.15))] \quad (A8)$$

where τ_s is surface tortuosity factor which accounts for the increase in diffusional length due to tortuous paths of real pores. Note that $D_{0,eff}$ is D_0/τ_s.

In the remainder of this section we compare the Knudsen and surface diffusion rates in a single pore. Consider a cylindrical and isothermal pore of radius a. The vapor diffusion rate due to Knudsen diffusion, $\dot{m}_K$, through the pore in the axial direction z is

$$\dot{m}_K = \pi a^2\left(-D_K \rho \frac{\partial m_1}{\partial z}\right) \quad (A9)$$

and due to surface diffusion, $\dot{m}_S$, on the surface of the pore is

$$\dot{m}_S = 2\pi a\left(-D_S \frac{\partial C_s}{\partial z}\right). \quad (A10)$$

Since C_s, surface concentration, is related to gel water content, W, and specific surface area, S_g, through $C_s = W/S_g$, the ratio of Knudsen diffusion and surface diffusion rates is

$$\frac{\dot{m}_K}{\dot{m}_S} = \frac{a}{2}\frac{D_K}{D_S} S_g \rho \left(\frac{\partial m_1}{\partial W}\right)_T. \quad (A11)$$

If we assume that the rates of adsorption and desorption of molecules are both large compared with the surface migration rates, the surface C_s and pore concentrations (ρm_1) will be almost in equilibrium, and hence will be related by the equilibrium adsorption isotherm, or

$$\rho m_1 = g(W, T, P).$$

The ratio of rates can be calculated knowing the properties of the gel. Table A2 contains the properties of both RD and ID gels and shows the results of the calculation of rate ratios. We see that surface diffusion dominates in a pore with RD gel characteristics while both mechanisms are important for a pore with ID gel characteristics.

Table A2. Surface and Knudsen diffusion rate comparison in a pore of silica gel at 30°C and 1 atm [11]

	Regular density	Intermediate density
Equilibrium relation	equation (41)	equation (42)
Heat of adsorption	equation (43)	equation (44)
Surface diffusivity	equation (A7)	equation (A7)
Knudsen diffusivity	equation (A2)	equation (A2)
ρ_p	$1129\ kg\ m^{-3}$	$620\ kg\ m^{-3}$
$\tau_s = \tau_g$	2.8	2.0
Pore surface area	$S_g = 7.8 \times 10^5\ m^2\ kg^{-1}$	$S_g = 3.40 \times 10^5\ m^2\ kg^{-1}$
Average pore radius	$a = 11\ Å = 11 \times 10^{-10}\ m$	$a = 68\ Å = 68 \times 10^{-10}\ m$
Range of water content	0.01–0.3 kg/kg	0.005–0.15 kg/kg
Range of ratio of Knudsen to surface diffusion rates	0.023–0.060	0.6–2.0

TRANSPORT D'HUMIDITE DANS LES LITS FIXES DE SILICAGEL—I. ETUDE THEORIQUE

Résumé—On étudie les mécanismes de diffusion de l'humidité dans les particules de silicagel. On trouve que pour le silicagel microporeux, la diffusion de surface est le mécanisme dominant du transfert d'humidité, tandis que pour le silicagel macroporeux les diffusions de Knudsen et de surface sont de même importance. On propose un modèle pour le transfert de chaleur et de masse dans un lit fixe mince, en prenant en compte les deux types de diffusion. En utilisant la méthode des différences finies pour résoudre les équations aux dérivées partielles, on calcule la réponse des lits minces de particules de silicagel à un changement en échelon des conditions à l'entrée d'air, et on compare au cas d'un modèle communément utilisé pour le dimensionnement des déshumidificateurs pour applications solaires de réfrigération avec dessicateurs.

FEUCHTIGKEITSTRANSPORT IM SILIKAGELBETT—I. THEORETISCHE UNTERSUCHUNG

Zusammenfassung—Untersucht wird der Mechanismus der Feuchtigkeitsdiffusion in Silikalgelpartikeln. Es zeigt sich, daß für feinporöses Silikagel die Oberflächendiffusion der dominierende Transportmechanismus für die Feuchtigkeit ist, während für makroporöses Silikagel die Diffusion nach Knudsen und die Oberflächendiffusion wichtig sind. Für den simultan verlaufenden Wärme- und Stofftransport in einem Dünnschichtbett von Trocknungspartikeln wird ein Modell vorgeschlagen, welches die Feuchtigkeitsdiffusion in die Partikel nach Knudsen und durch Oberflächendiffusion berücksichtigt. Zur Lösung der partiellen Differentialgleichung wird die Methode der Finiten-Differenzen benutzt, um Voraussagen über das Verhalten von Silikagelpartikeln bei schrittweiser Veränderung der Zuluftzustände im Dünnschichtbett zu machen. Dies wurde mit einem Modell verglichen, welches—nur scheinbar—gasseitig gesteuert ist und normalerweise für die Auslegung von Trockenentfeuchtern zur solaren Trockenkühlung Anwendung findet.

ПЕРЕНОС ВЛАГИ В ПЛОТНЫХ СЛОЯХ СИЛИКАГЕЛЯ—I. ТЕОРЕТИЧЕСКОЕ ИССЛЕДОВАНИЕ

Аннотация—Исследуются механизмы диффузии в частицах силикагеля. Установлено, что в случае микропористого силикагеля поверхностная диффузия является основным механизмом переноса влаги, в то время как для макропористого силикагеля одинаково существенна как кнудсеновская, так и поверхностная диффузия. Предложена модель совместного тепло- и массообмена в тонких плотных слоях частиц-осушителей, описывающая кнудсеновскую и поверхностную диффузию в частицах. С помощью конечно-разностных методов решения полученных дифференциальных уравнений в частных производных рассчитана чувствительность тонких слоев частиц силикагеля на ступенчатые изменения условий подачи воздуха и проведено сравнение с псевдо-газовой моделью, обычно применяемой при проектировании осушителей для охлаждения установок с использованием солнечной энергии.